

This document is the author's final manuscript of

M. Collet, M. Ouisse, M. Ichchou & R. Ohayon: Semi-active optimization of 2D wave dispersion into shunted piezo-composite systems for controlling acoustic interaction. *Smart Materials and Structures*, 2012.

This paper has been published by Elsevier and can be found at
<http://dx.doi.org/10.1088/0964-1726/21/9/094002>

Semi-active optimization of 2D wave's dispersion into shunted piezocomposite systems for controlling acoustic interaction

M Collet¹ and M Ouisse¹ and MN Ichchou² and R. Ohayon³

¹ FEMTO-ST, Applied Mechanics Department, UMR-CNRS 6174, 24 chemin de l'épitaphe, 25000 Besançon, France

² LTDS UMR-CNRS 5513, École Centrale de Lyon, 36 avenue Guy de Collongue, 69134 Écully, France

³ SMCS Lab, Conservatoire National des Arts et Metiers, 2 rue Conté, 75141 Paris Cedex 03, France

E-mail: manuel.collet@univ-fcomte.fr, morvan.ouisse@univ-fcomte.fr, Mohamed.Ichchou@ec-lyon.fr, roger.ohayon@cnam.fr

Abstract. Based on recent works on application of Floquet-Bloch theorem to periodical mechanical systems including frequency-dependent parameters [1], we propose in this paper an extension to vibroacoustic behavior analysis of smart structures. The objective is to optimize electronic circuits used to shunt some piezoelectric patches distributed on the structure, in order to minimize the acoustic radiation of the structure. The proposed approach is based on the computation of the multi-modal wave dispersion curves into the whole first Brillouin zone of the structure, and associated propagation characteristics in the acoustic fluid. The impedance of the shunt circuit is then optimized in order to render the acoustic waves evanescent. This work is a collaborative effort supported by the French Research Agency under grant number *NT09* – 617542.

1. Introduction

The concept of metamaterial is presented in this paper, based on the coupling of two strategies for vibroacoustic control. The first one is related to periodic structures theories usually connected to metamaterial developments. In this case, it is well known that the dynamic behavior is fully connected to periodicity ratios, while corresponding pass bands and blocked bands can be of real use in vibration control. The second concept is associated to vibration control through piezoelectric and smart materials. Specifically, shunted piezoelectric smart materials are employed for the metamaterial achievement by integrating into the metamaterial electronics and numerical components allowing implementation of adaptive and controlled behavior. The notion of programmable matter within the meaning of work presented in [2] is extended to vibroacoustic programming. The paper main novelty is then the design through full numerical analyses of a smart structure [1] with broad band control abilities. Wave based methods and numerical simulation tools are adapted to the proposed concept. The metamaterial efficiency is illustrated from the low frequency range to the mid frequency band as well. Development of a wave trap metamaterial can be the ultimate goal of the reported research and results.

2. Piezo-elasto-dynamical application of the Floquet-Bloch theorem

The metamaterial considered in this paper are illustrated in figure 1. The generic piezocomposite cell is first used for the optimization of electrical shunt $Z(\omega)$ by considering an infinite periodic distribution of the cells, and finally validated in the context of the integration of a finite structure.

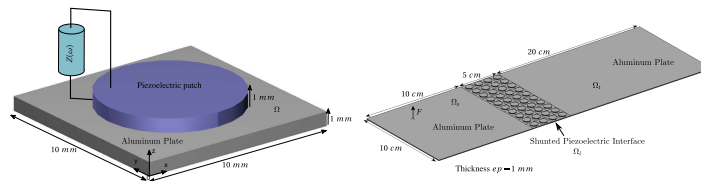


Figure 1: Generic 3D piezocomposite periodic cell (left); Integration of the smart interface in finite structure (right)

2.1. Numerical Computation of the Bloch's waves

The Floquet-Bloch approach [3, 4] has been widely used for developing homogenization techniques and spectral asymptotic analyses like in the work of [5]. Nevertheless these approaches have been only developed for undamped or lightly damped mechanical systems. In these cases, most of the published works present techniques based on the

mesh of a real k -space following the boundary of the first Brillouin zone for obtaining the corresponding dispersion curves and the associated Floquet vectors. For undamped systems, only propagative or evanescent waves exist corresponding to a family of eigen solutions purely real or imaginary. Discrimination between each class of waves is easy. If a highly damped system (whose FE matrices are complex and frequency dependent) and a frequency-dependent electrical shunt impedance are considered, the obtained eigenvalue problem is not quadratic and a complex specific numerical methodology has to be implemented. Furthermore, evanescent parts of propagating waves appear as the imaginary part of pulsation. It then becomes much more difficult to distinguish the propagative and evanescent waves as all solution appear complex.

Another much more suitable possibility for computing damped system, dedicated for time/space deconvolution and for computation of diffusion properties as defined in [1, 6, 7], is to transform the discretized form of the weak formulation into the following generalized eigenvalue problem [1]:

$$0 = \begin{bmatrix} K(Z(\omega)) - \omega^2 M + \lambda_n(\omega, \phi)L(\phi, Z(\omega)) \\ -\lambda_n^2(\omega, \phi)H(\phi, Z(\omega)) \end{bmatrix} \mathbf{u}_n(\omega, \phi), \quad (1)$$

where $\lambda = ik$, (k being the wave number), M and $K(Z(\omega))$ are respectively the standard symmetric semi-definite mass and stiffness matrices (the mass matrix is semi definite because electrostatic equation are condensed [8, 9]), Z is the impedance of the shunt circuit, $L(\phi, Z(\omega))$ is a skew-symmetric matrix, ϕ represents the direction angle into the reciprocal 2D lattice domain and $H(\phi, Z(\omega))$ is a symmetric semi-definite positive matrix. \mathbf{u}_n is the generalized eigen vector defined on all degrees of freedom of the used finite element model.

In this problem, the pulsation ω is a real parameter corresponding to the harmonic frequency. Wave's numbers and Floquet vectors are then computed. An inverse Fourier transformation in the k -space domain can be used to evaluate the physical wave's displacements and energy diffusion operator when the periodic distribution is connected to another system [6]. Another temporal inverse Fourier transformation can furnish a way to access spatio-temporal response for non-homogeneous initial conditions. As L is skew-symmetric, the obtained eigen values are quadruple $(\lambda, \bar{\lambda}, -\lambda, -\bar{\lambda})$ collapsing into real or imaginary pairs (or a single zero) when all matrices are real (i.e. for an undamped system). In this case a real pair of eigen values correspond to evanescent modes oriented in two opposite directions in the k -space and imaginary values to two traveling waves propagating in opposite directions [10].

2.2. Computation of the evanescence and damped power flow criteria

One aim of this paper is to provide a numerical methodology for optimizing the piezoelectric shunt impedance $Z(\omega)$ for controlling energy flow into the periodically distributed piezo-composite structure. Suitable criteria are then required.

The first criterion which is considered for describing the ability of the metacomposite to transmit structural energy is based on the computation of the wave group velocities. Indeed, they indicate how energy is transported into the considered system and allow to distinguish the 'propagative' and 'evanescent' waves. If a Bloch eigen solution is considered, the associated group velocity vector [11] is given by:

$$\mathbf{C}_{g_n}(\omega, \phi) = \nabla_{\mathbf{k}\omega} = \frac{\langle\langle \mathbf{S} \rangle\rangle}{\langle\langle e_{tot} \rangle\rangle} = \frac{\langle \mathbf{I} \rangle}{\langle E_{tot} \rangle} \quad (2)$$

where $\langle\langle : \rangle\rangle$ is the spatial and time average respectively on one cell and one period, \mathbf{S} is the density of energy flux, \mathbf{I} the mean intensity and e_{tot} , E_{tot} the total piezomechanical energy and its time average on a period (see [11] for details). In this problem, only mechanical energy transportation is considered as the electrostatic coupling is decentralized on each cell and can not induce spatial energy transportation. The intensity vector \mathbf{I} is computed by:

$$\langle \mathbf{I} \rangle = -\frac{\omega}{2} \text{Re} \left(\int_{\Omega_x} C(\varepsilon_n(\mathbf{x}, \omega, \phi) + ik\Xi_n(\mathbf{x}, \omega, \phi)) \cdot (\mathbf{w}_n^*(\mathbf{x}, \omega, \phi)) \frac{d\Omega}{V_{ol}} \right) \quad (3)$$

where $*$ is the complex conjugate and V_{ol} the domain volume. The group velocity vectors $\mathbf{C}_{g_n}(\omega, \phi)$ is computed for all wave numbers at each frequency. In order to focus the analysis only on flexural modes (S and SH ones), an index $Ind(n, \omega, \phi)$ is computed for each mode, frequency and angle value, quantifying the ratio of the kinetic energy associated to transverse displacement to the total energy of the structure. The optimization of the shunt impedance $Z(i\omega)$ is based on the following criterion:

$$\text{Crit}_1(Z(i\omega), \phi) = \max_{n/Ind(n, \omega, \phi) > 0.8} (\mathbf{C}_{g_n}(\omega, \phi) \cdot \Phi). \quad (4)$$

The second criterion which is considered is based on the maximization of the damped electric power $P_{elec}(n, \omega, \phi)$. In order to increase damping effect inside the smart metamaterial, this term needs to be sufficiently large. The corresponding criteria is

$$\text{Crit}_2(Z(i\omega), \phi) = \max_{n/Ind(n, \omega, \phi) > 0.8} \frac{1}{P_{elec}(n, \omega, \phi)}. \quad (5)$$

2.3. Computation of the sound radiation efficiency

The sound radiation efficiency of a plate depends on the coupling of sound waves in the air and flexural waves (vibration) in the plate. Optimal efficiency (maximum energy transfer from vibration to sound or vice versa) is achieved when the plate vibrates such that the wavelength of flexural waves in the plate is equal to the wavelength of acoustic waves in the air. This is more commonly known as the coincidence frequency of radiation [12]. The corresponding frequency value can be obtained through the computation of the kz_n value of the induced acoustic wave number. If one considers an infinite plate in which an harmonic plane wave is propagating with a wave number kx_n at pulsation ω , as the acoustic pressure radiated from this infinite system is a solution of the Helmholtz

equation, coupled by considering interface continuous normal velocity, the expression of kz_n is:

$$kz_n = \sqrt{\left(\frac{\omega}{c}\right)^2 - kx_n^2}, \quad (6)$$

where c is the speed of sound in the acoustic medium. This expression is classical for the analysis of radiation of infinite plates and is used to define the coincidence frequency that distinguishes evanescent and propagative acoustic waves [12].

3. Optimization of the Flexural energy flow inside the shunted periodic piezo-composite

The considered piezo-composite cell is presented in figure 1. The supporting plate material is standard aluminum with 0.1 % of hysteretic damping ratio.

3.1. Optimization of the waves group velocities by using \mathbf{Crit}_1

In this part, optimization of the transmission capability of the designed adaptive metacomposite is considered by using \mathbf{Crit}_1 (4). The objective is to avoid any energy transportation when flexural waves are excited into the periodically distributed shunted piezocomposite cells. The numerical optimization procedure is based on a multidimensional unconstrained nonlinear minimization algorithm. The optimization is done by considering an active/reactive electronic circuit through a complex impedance $Z(\omega)$.

The analysis is initialized with an arbitrary complex value of the shunt impedance. Optimization steps are then proceeded using criterion \mathbf{Crit}_1 by considering any frequency dependent complex impedance for describing the circuit behavior.

Figure 2 shows the dispersion curves of the wave numbers along x axis for $\phi = 0$, and z component of acoustic wave number, for both initial and optimal impedance shunts.

It must be underlined that the procedure has the ability to catch all Bloch's solutions including evanescent ones that generally do not appear in literature because of their imaginary character. In the context of structural dynamics, including damping effects is mandatory for real-life applications and all wave numbers become complex, which constitutes a key point in the analysis [1, 10]. For a sake of clarity, the following results are presented by exhibiting only propagative waves responsible for energy transport, using a suitable wave filter based on the group velocity. It then becomes easy to observe branches similar to standard S_0 , A_0 , A_1 , TH waves. It can immediately be observed that the optimization of the shunt impedance leads to a large decrease of the group velocity of the A_0 mode while the A_1 wave, which becomes propagative at 8.8 kHz, is not controlled by the optimal configuration. The bending waves also propagate energy with a very low velocity and can be considered as evanescent. Flexural energy is, then, only transported by the A_1 mode after the cutting frequency.

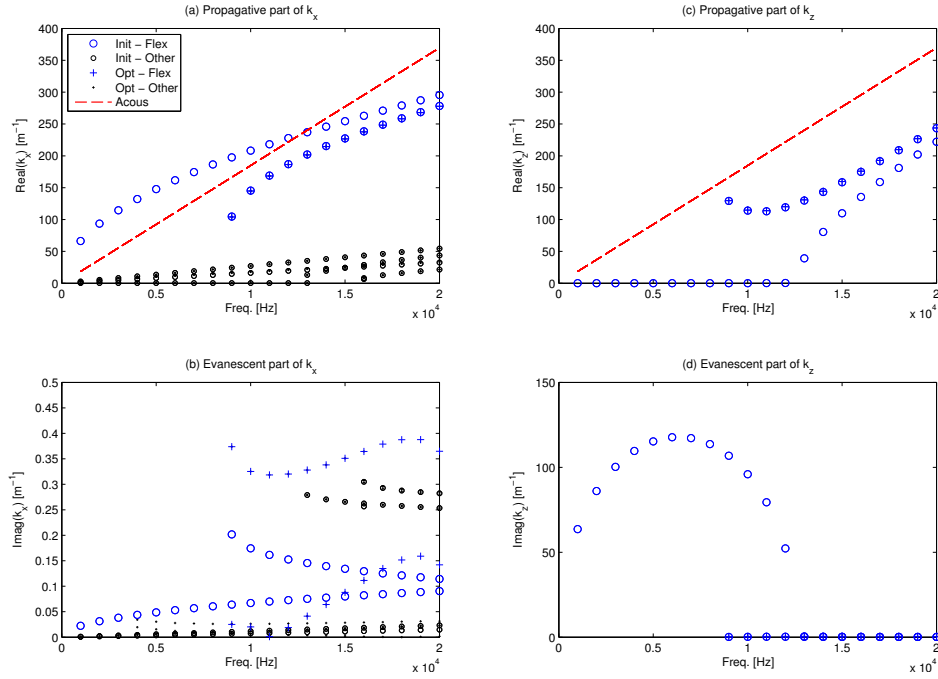


Figure 2: On the left, Real (a) and imaginary (b) parts of the wave number $kx_n(i\omega)$ of plane waves propagating into the smart plate along (Ox) axis and, on the right, the corresponding real (a) and imaginary (b) parts of the acoustic out plane wave number kz_n .

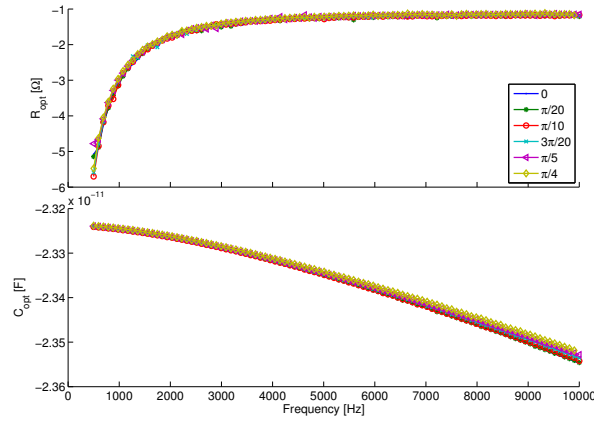


Figure 3: Real and imaginary parts of the optimal impedance

The propagative part of the controlled wave is strongly modified: from two complex conjugated solutions, the A_0 wave changes after control to 4 solutions (2 complex conjugates and their opposites). This situation is described in [10], it corresponds to high order evanescent waves solutions. On the same figure, the acoustic performance of the system is also presented. The acoustic dispersion curve is represented in red, and it can be observed that the first flexural mode, in the initial configuration, is propagative

above the coincidence frequency, which is a classical behavior. The interesting point here is that the optimized configuration cancels the radiation of this wave, since it becomes fully evanescent after optimal choice of the shunt impedance.

The real and imaginary parts of the optimal impedance are plotted in figure 3 for all angles. The optimal impedance values almost correspond to a constant negative capacitance in all directions. The corresponding average value is -233.66 pC/V . Equivalent resistances corresponding to the active part of the shunt impedance are negative which indicates that the optimization leads to provide energy to the system for controlling mechanical damping effects introduced by hysteretic damping in the model. The optimized configuration tends to converge towards a fully conservative system. The mean value of the resistance is -1.5319Ω , and the electrical dissipated energy appears negative when the optimal shunt is connected to the patch.

3.2. Optimization of damped power flow inside the electric shunts by using \mathbf{Crit}_2

Another strategy for optimizing the adaptive metacomposite consists in focusing on the damped power flow inside the electric shunts by using the criterion \mathbf{Crit}_2 . In this case the objective is to improve the absorption ability of the smart structure. Figure 4 shows the dispersion curves of the wave numbers along x axis for $\phi = 0$, and z component of acoustic wave number, for both initial and optimal impedance shunts. The optimal impedances of the electric shunts are plotted in figure 5 for various values of ϕ .

The first observation is that the optimization of the shunt impedance for improving the absorption characteristics of the system induces modifications of the group velocities of the controlled waves, while the propagative part of the wave numbers remain unchanged. This can be explained by a large improvement of the ratio between the real and imaginary parts of the waves numbers, which physically corresponds to the forcing of propagating effects to increase damping effects: energy can propagate inside the periodically distributed set of active cells for allowing electrical energy conversion. The dissipated power is largely increased when optimal shunt is connected to the patch. On the same figure, the acoustic performance of the system is also presented. The acoustic dispersion curve is represented in red, and the behavior of the initial configuration is unchanged. Contrarily to the optimization using \mathbf{Crit}_1 , the first flexural mode still propagates in the optimized system. The main difference with the initial configuration lies in the fact that the evanescent part of the acoustic wave number is much higher, which indicates that the acoustic wave is damped, exhibiting a decay rate which is related to the imaginary part of the wave number. This is in accordance with the objective, which tends to add damping in the system, instead of changing the nature of the flexural mode.

The optimal impedance values (figure 5) correspond to an almost constant negative capacitance in all directions. The average value is -237.43 pC/V . Equivalent resistances corresponding to the active part of the shunt impedance are positive, which

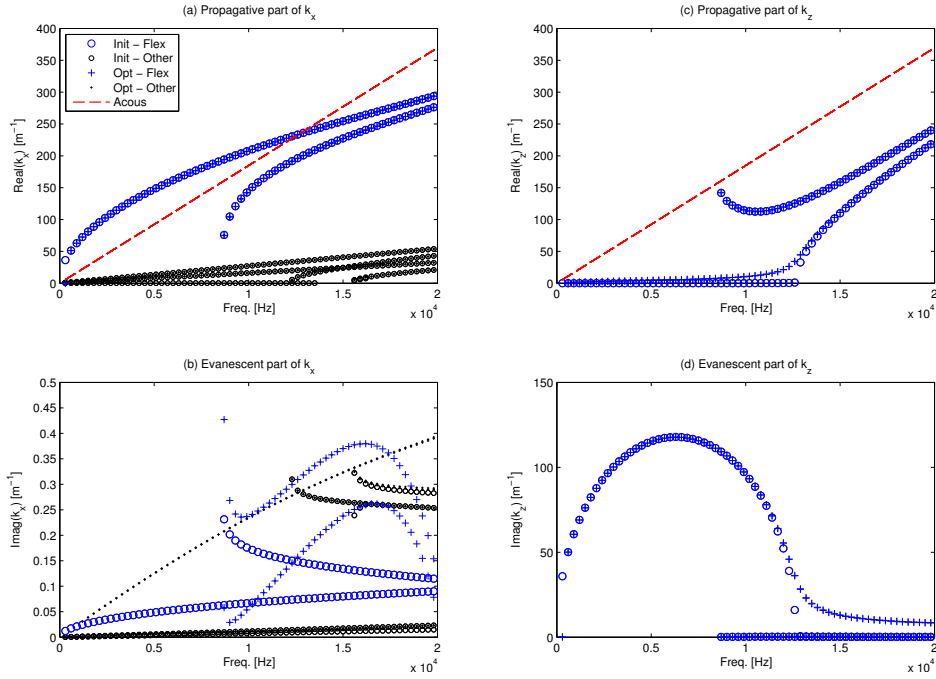


Figure 4: On the left, real (a) and imaginary (b) parts of the wave number $kx_n(i\omega)$ of plane waves propagating into the smart plate along (Ox) axis and, on the right, the corresponding real (a) and imaginary (b) parts of the acoustic out plane wave number kz_n .

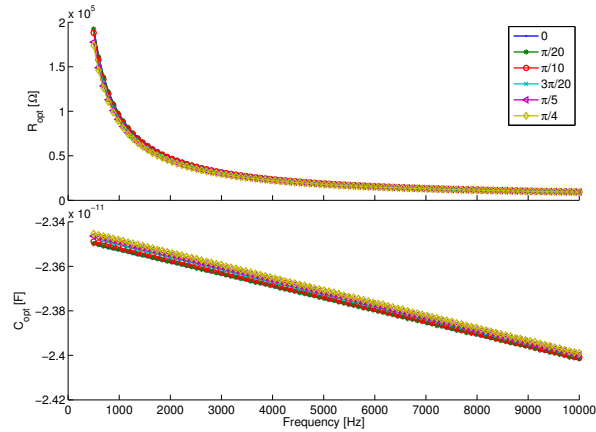


Figure 5: Real and imaginary parts of the optimal impedance

is in accordance with the fact that a damping effect is awaited.

4. Validation on a periodically semi-distributed set of adaptive cells

4.1. Mechanical interface characterization

Up to that point, the optimizations of the smart metacomposite which have been proposed were performed by considering infinite periodic structures. The objective of this section is to illustrate the applicability of the designs for integration into real-life finite structures. The optimal impedance is then applied on a finite set of shunted piezo-composite cells distributed on a part of a totally free plate system submitted to a point force in one corner, as described in figure 1. Material damping is introduced throughout a constant imaginary part of the elasticity tensor of 0.1%. The harmonic response of this system is then computed on the [500, 10000] Hz frequency band when optimal impedances, obtained by criteria $Crit_1$ or $Crit_2$, are connected or not to each patches.

From the observation of figures 6, the main particularities of the synthesized optimal impedances can be emphasized. The first configuration, obtained by using $Crit_1$, leads the adaptive interface to avoid any flexural energy transfer. The mechanical response of the system is strongly modified, and the resonance peaks are moved far from the open circuit response, which indicates a modification of the internal dynamics. The second configuration, based on $Crit_2$ optimal shunt, forces energy dissipation into the resistive part of the electric shunt. In that case, the conservation of the modal architecture into the energy spectrum can be observed, even if some damping effects limit the peak's amplitudes.

The minimization of the flexural wave group velocity $Crit_1$ leads to decrease the part of kinetic energy transmitted to the non-excited part of the plate located behind the adaptive interface as shown in figure 7 while the maximization of the damped energy $Crit_2$ only slightly modify this distribution. The modification of the energy distribution into the system is very important after 6 kHz and increase with the frequency when the energy is globally transported by A_0 mode. This is not the case in the lower frequency band when the interface works in the near field domain of the applied point force.

Finally these results indicate that the smart metacomposite interface changes the system admittance and filter wave diffusion by increasing its reflexivity properties. The energy diffusion is also clearly condensed into the left part of the system with a large decrease of the amplitude compared to the one obtained with open circuit and $Crit_2$ optimal shunt. With this type of shunt something similar to a wave trap effect can be observed. With $Crit_2$ optimal shunt, an improvement of the damping effect leading to vibration attenuation can be observed, without wave trap behaviour.

4.2. Acoustical radiated power flow

Figure 8 shows the acoustic power radiated by right end part of the system Ω_t , in terms of power levels, for the initial configuration and for both optimal shunts. The global

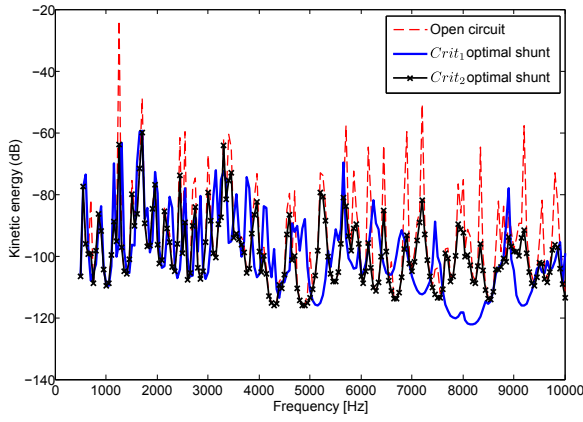


Figure 6: Mean value of the kinetic energy on the whole domain Ω with open circuit (red dashed line), $Crit_1$ (blue line) and $Crit_2$ (black marked line) optimal shunt connected to piezoelectric patches

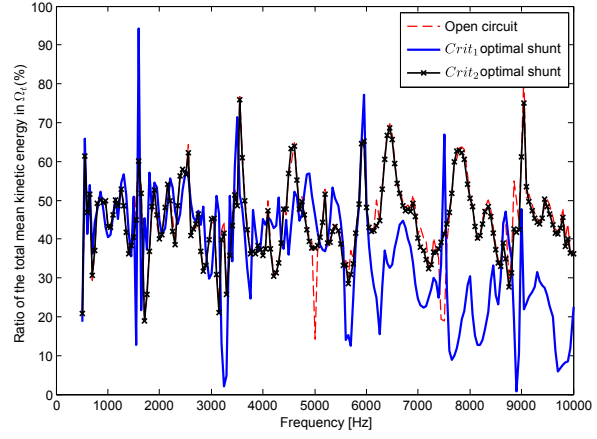


Figure 7: Ω_t ratio of the total kinetic energy mean value in percent with open circuit (red dashed line), $Crit_1$ (blue line) and $Crit_2$ (black marked line) optimal shunt connected to piezoelectric patches

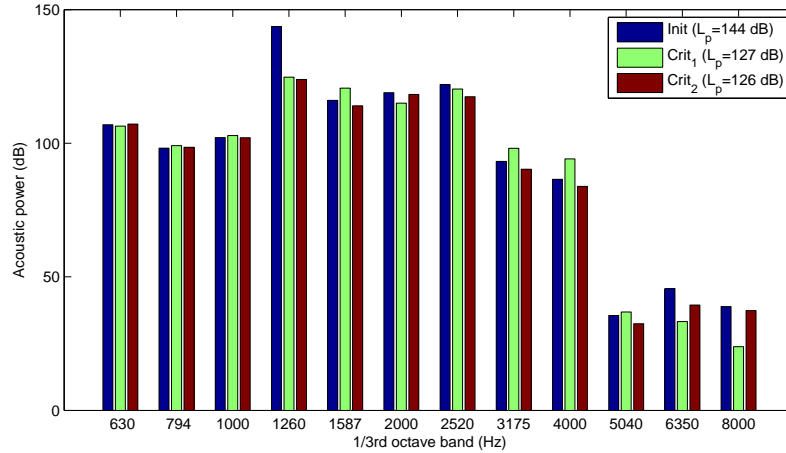


Figure 8: Acoustic power flow radiated by the right free part of the composite plate Ω_t

acoustic level reduction is almost the same for the two optimal shunts (17 dB), and it is mostly due to a high reduction in the 1260Hz third octave band where is located one emitted mode. For other frequency bands before 5040 Hz, the reduction is generally small (maximum 3 dB), or even negative in some cases. The reduction of vibration level does not always lead to reduction of acoustic power since it reorganizes the distribution of the displacement field on the structure, which means that the optimal configuration can correspond to a more efficient field in terms of acoustic radiation in frequency band initially dominated by non emitted response. In the high frequency bands, we observe a strong reduction up to 15 dB when the metacomposite interface is controlled by using optimal shunt obtained with $Crit_1$. This behavior is induced by the strong reduction in

the vibration transmissibility already observed in figure 7. The next part of this work will consider an acoustic-based criteria for optimization of the electric shunts, in order to reach higher acoustic efficiency.

5. Conclusions

This paper presents a numerical procedure able to compute the damped wave's dispersion functions in the whole first Brillouin domain of multi dimensionnal piezo-elastodynamical wave guides. The method is applied for determining the optimal impedance allowing to minimize the group velocities of the flexural waves. Based on this approach, some numerical tests on a finite dimension system incorporating a semi-distributed set of shunted piezo-composite cells have been performed. A strong influence of the designed shunt circuits in the vibroacoustic response of the system is underlined. The proposed numerical procedures can be used for optimizing the energy diffusion operator of adaptive mechanical interface, even if additional work has to be done for optimizing the complete interface scattering and for controlling the evanescent waves playing an important role in the dynamical response of a finite system incorporating semi-distributed interface. Another part of this future developments should deal with the full vibroacoustic optimization incorporating a strong fluid-structure coupling effect. The proposed methodology can also be used for the analysis of particular dissipation phenomenon such as those induced by complex shunted piezoelectric patches [13, 14], or even foams or complex polymers behaviors.

References

- [1] Collet M, Ouisse M, Ruzzene M and Ichchou M 2011 *International Journal of Solids and Structures* **48** 2837–2848
- [2] Toffoli T and Margolus N 1991 *Physica D: Nonlinear Phenomena* **47** 263 – 272 ISSN 0167-2789
- [3] Floquet G 1883 *Annales de l'Ecole Normale Supérieure* **12** 47–88
- [4] Bloch F 1928 *Zeitschrift für Physik* **52** 550–600
- [5] Allaire G and Congas C 1998 *Journal de Mathématiques Pures et Appliquées* **77** 153–208
- [6] Collet M, Cunefare K and Ichchou N 2009 *Journal of Int Mat Syst and Struct* **20** 787–808
- [7] Houillon L, Ichchou M and Jezequel L 2005 *Journal of Sound and Vibration* **281** 483–507 ISSN 0022-460X
- [8] Hagood N W and von Flotow A H 1991 *Journal of Sound and Vibration* **146(2)** 243–268
- [9] Collet M and Cunefare K 2008 *Journal of Int Mat Syst and Struct* **19** 1251–1271
- [10] Garvic L 1995 *Journal of Sound and Vibration* **185** 531–543
- [11] Maysenhölder W 1994 *Körperschall-energie Grundlagen zur Berechnung von Energiedichten und Intensitäten* (Wissenschaftliche Verlagsgesellschaft, Stuttgart)
- [12] Fahy F and Gardonio P 2007 *Sound and structural vibration: radiation, transmission and response* (Academic press)
- [13] Beck B, Cunefare K and Ruzzene M 2008 Broadband vibration suppression assessment of negative impedance shunts *Proceedings of SMASIS08* vol 6928 (ASME)
- [14] Casadei F, Ruzzene M, Beck B and Cunefare K 2009 Vibration control of plates featuring periodic

arrays of hybrid shunted piezoelectric patches *Proceedings of SPIE - Smart Structures and Materials* vol 7288 (SPIE)